3. Iwasaki Y. Pathology of chronic myelopathy associated with HTLV-I infection (HAM/TSP). J Neurol Sci 1990;96:103–123.
4. Umehara F, Osame M. Histological analysis of HAM/TSP pathogenesis. In: Sugamura K, Uchiyama T, Masao M, Kannagi M, eds. Two decades of adult T-cell leukemia and HTLV-I research. Tokyo: Japan Scientific Societies Press, 2003:141–148.
5. Vine AM, Witkover AD, Lloyd AL, et al. Polygenic control of human T lymphotropic virus type I (HTLV-I) provirus load and the risk of HTLV-I-associated myelopathy/tropical spastic paraparesis. J Infect Dis 2002; 186:932–939.
6. Jeffery KJ, Usuku K, Hall SE, et al. HLA alleles determine human T-lymphotropic virus-I (HTLV-I) proviral load and the risk of HTLV-I-associated myelopathy. Proc Natl Acad Sci USA 1999;96:3848–3853.
7. Jeffery KJ, Siddiqui AA, Bunce M, et al. The influence of HLA class I alleles and heterozygosity on the outcome of human T cell lymphotropic virus type I infection. J Immunol 2000;165:7278–7284.
8. Osame M. Review of WHO Kagoshima meeting and diagnostic guidelines for HAM/TSP. In: Blattner WA, ed. Human retrovirology: HTLV. New York: Raven Press, 1990:191–197.
9. Furukawa Y, Yamashita M, Usuku K, et al. Phylogenetic subgroups of human T cell lymphotropic virus (HTLV) type I in the tax gene and their association with different risks for HTLV-I-associated myelopathy/tropical spastic paraparesis. J Infect Dis 2000;182:1343–1349.
10. Nagai M, Usuku K, Matsumoto W, et al. Analysis of HTLV-I proviral load in 202 HAM/TSP patients and 243 asymptomatic HTLV-I carriers: high proviral load strongly predisposes to HAM/TSP. J Neurovirol 1998;4:586–593.
11. Tajima Y, Kishimoto R, Sudoh K, et al. Spinal magnetic resonance image alterations in human T-lymphotropic virus type I-associated myelopathy patients before and after immunomodulating treatment. J Neurol 2003;250:750–753.
12. Shakudo M, Inoue Y, Tukada T. HTLV-I-associated myelopathy: acute progression and atypical MR findings. AJNR Am J Neuroradiol 1999; 20:1417–1421.
13. Watanabe M, Yamashita T, Hara A, et al. High signal intensity in the spinal cord on T2-weighted images in rapidly progressive tropical spastic paresis. Neuroradiology 2001;43:231–233.
14. Levin MC, Lehky TJ, Fierlage AN, et al. Immunologic analysis of a spinal cord-biopsy specimen from a patient with human T-cell lymphotropic virus type I-associated neurologic disease. N Engl J Med 1997;336:839–844.
15. Kiwaki T, Umehara F, Arimura Y, et al. The clinical and pathological features of peripheral neuropathy accompanied with HTLV-I associated myelopathy. J Neurol Sci 2003;206:17–21.

AIDS RESEARCH AND HUMAN RETROVIRUSES
Volume 20, Number 10, 2004, pp. 1092–1099

Human T Cell Lymphotropic Virus Type I (HTLV-I) $p12^I$ Is Dispensable for HTLV-I Transmission and Maintenance of Infection *in Vivo*

YOSHITAKA FURUKAWA,[1] KOICHIRO USUKU,[2] SHUJI IZUMO,[3] and MITSUHIRO OSAME[4]

ABSTRACT

The function of the $p12^I$ protein of human T cell lymphotropic virus type I (HTLV-I) has been under debate. p12K (lysine) and p12R (arginine) variants of this protein at amino acid 88 and a shorter life of p12K had been reported by another group. Because HTLV-I-associated myelopathy/tropical spastic paraparesis (HAM/TSP) patients usually have a higher provirus load than asymptomatic HTLV-I carriers (ACs), and $p12^I$ had been suggested to confer a proliferative effect on HTLV-I-infected cells *in vitro*, it is possible that the relatively unstable p12K is less frequent in HAM/TSP patients than in ACs. To elucidate whether p12K and other alterations in the *p12* gene were related to the outcome of HTLV-I infection, we sequenced the *p12* gene in 144 HAM/TSP patients, 41 adult T cell leukemia (ATL) patients, and in 46 ACs. p12K was observed in only two HAM/TSP patients, but was not present in either ATL patients or ACs. Interestingly, a premature termination codon in the *p12* was observed in 5.6% of HAM/TSP patients and in 4.9% of ATL patients but none was found in ACs. The *p12* initiation codon was destroyed in one HAM/TSP patient. These HTLV-I variants with truncated p12 protein or with a destroyed initiation codon in the *p12* gene appeared to have been transmitted in the subjects' families. These findings suggest that *p12* is dispensable for the transmission and maintenance of HTLV-I infection, although it is premature to conclude that sequence varitation in the *p12* gene is associated with differences in the outcome of HTLV-I infection.

INTRODUCTION

HUMAN T CELL LYMPHOTROPIC VIRUS TYPE I (HTLV-I) was first isolated from a cutaneous T-lymphoma in 1980,[1] and was determined to be the etiological agent of adult T cell leukemia (ATL).[2] In 1985 an association was reported between tropical spastic paraparesis, which had been considered to be a degenerative disorder, and HTLV-I.[3] In 1986 HTLV-I was reported to be associated with a similar syndrome, which was called HTLV-I-associated myelopathy (HAM);[4] the condition is now called HAM/TSP. One of the intriguing questions associated with HTLV-I infection is why the same HTLV-I causes two distinct diseases. Another question is why only a small proportion of infected people, approximately 2–3%, develop ATL,[5] and a further 0.25% develop HAM/TSP in Japan,[6] while the majority (about 97%) of HTLV-I-infected individuals develop no associated disease. To date, HTLV-I provirus isolated from ATL and HAM/TSP patients was reported to be indistinguishable in the LTR and env regions.[7] However, we recently reported the existence of subgroups in the *tax* gene and different risks of HAM/TSP among different HTLV-I subgroups.[8] Tax is a multifunctional protein encoded by the open reading frame IV of the pX region of HTLV-I that can transactivate HTLV-I transcription through LTR.[9] Tax can also transactivate many

[1]Division of Blood Transfusion Medicine and Cell Therapy, Kagoshima University Hospital, 8–35–1 Sakuragaoka, Kagoshima 890–8520, Japan.
[2]Department of Medical Informatics, Faculty of Medicine, Kagoshima University, Kagoshima, Japan.
[3]Center for Chronic Viral Diseases, Faculty of Medicine, Kagoshima University, Kagoshima, Japan.
[4]Department of Neurology and Geriatrics, Kagoshima University Graduate School of Medical and Dental Science, Kagoshima, Japan.

cytokine genes[10,11] and protooncogenes.[12] These observations raise the interesting possibility that differences in Tax may influence the outcome of HTLV-I infection. $p12^I$ is another protein encoded by the open reading frame I of the pX region, the function of which is not well elucidated.[13] The $p12^I$ protein can bind to the 16-kDa subunit of the H^+-ATPase proton pump[14] and to the β and γc chains of the interleukin 2 (IL-2) receptor.[15] Although $p12^I$ does not influence the infectivity of HTLV-I in *in vitro* culture, it has been suggested that $p12^I$ is necessary for persistent HTLV-I infection in the rabbit model.[16] When $p12^I$ was expressed under experimental conditions, $p12^I$ was reported to reside in the endoplasmic reticulum and Golgi,[17] and to be associated with several proteins such as calcium-binding protein,[18] and free major histocompatibility complex class I heavy chain (MHC-I-Hc).[19] Association of $p12^I$ with calreticulin modulates activation of nuclear factor of activated T cells, and enhances STAT5 activation.[20] Binding of the $p12^I$ with MHC-I-HC was shown to result in a significant decrease in the surface level of MHC-I on human T cells.[19] These previously reported findings suggested that $p12^I$ might confer a proliferative advantage on HTLV-I-infected cells and also may affect the result of HTLV-I infection.

The $p12^I$ protein with lysine in the C-terminal region (position 88: p12K) was shown to be a substrate for ubiquitylation and degradation by the proteasome. Also, the p12K variant has a half-life significantly shorter than that of $p12^I$ with arginine in the same position (p12R).[21] There have been conflicting results concerning the prevalence of these p12K and p12R alleles in HAM/TSP patients and asymptomatic carriers (ACs). p12K was reported to be more frequent in HAM/TSP patients than in ACs in one study.[21] Another study reported that p12K was observed in a small minority of both HAM/TSP patients and ACs.[22] Although it had been suggested that $p12^I$ confers a proliferative advantage of HTLV-I-infected cells *in vitro*, the effect of $p12^I$ *in vivo*, if it is indeed expressed, may be different. If p12K, which is more unstable than p12R, is more frequently observed in HAM/TSP patients (who usually have a higher HTLV-I provirus load) than in ACs, one possibility is that a shorter life of p12K is associated with greater proliferation of HTLV-I-infected cells *in vivo*. We therefore set out to examine whether the p12K variant is present at a significantly higher frequency in HAM/TSP patients than in ACs in Japan, and whether the p12R/K allele was associated with the HTLV-I tax viral genotype, that we previously reported influenced the risk of HAM/TSP development in this Japanese population. We then extended our study to examine other variations in the *p12* gene, to test whether $p12^I$ is dispensable for HTLV-I infection in humans, and whether variations in the *p12* gene were associated with different risks of HTLV-I-associated diseases. We discuss the role of $p12^I$ in the establishment of stable infection in humans, and the association between sequence variations in the *p12* gene of HTLV-I and HTLV-I-related diseases.

MATERIALS AND METHODS

Study population

One hundred and forty-four cases of HAM/TSP were compared with 41 ATL patients (30 acute type, 3 lymphoma type, 6 chronic type, and 2 smoldering type ATL) and 46 randomly selected HTLV-I-seropositive asymptomatic blood donors (ACs). All cases and controls were of Japanese ethnic origin and resided in Kagoshima prefecture, Japan. The diagnosis of HAM/TSP was made according to the World Health Organization diagnostic criteria.[23] The diagnosis and clinical subtype of ATL were made according to Shimoyama's criteria.[24] Asymptomatic carriers were randomly selected from 111 individuals who were notified by the Red Cross following blood donation that they were infected with HTLV-I and subsequently attended our clinic.[25]

Sequencing of HTLV-I p12 gene

All DNA samples extracted from peripheral blood mononuclear cells (PBMCs) were sequenced from position 6801–7199 (numbered as in the reference strain ATK),[26] which included the entire HTLV-I *p12* gene (nucleotides 6834–7130). Polymerase chain reaction (PCR) was done on the extracted DNA to amplify proviral DNA, and nucleotide sequences were determined in both directions. One hundred nanograms of DNA was amplified by 35 cycles of PCR using Expand high fidelity PCR system (Boehringer Mannheim, Japan) and 1 μM primers [ORFI03$^+$: 5′-CGTCAGATACCCCCATTACTC-3′ (6598–6619) and ORFI02$^-$: 5′-AGCCGATAACGCGTCCATCGAT-3′ (7472–7493)]. Each PCR cycle consisted of denaturation at 94°C for 60 sec, annealing at 58°C for 75 sec, extension at 72°C for 90 sec, and extension of the final cycle at 72°C for 10 min. Amplified DNA products were purified using the QIA quick purification kit (Qiagen, Japan) and 0.1 μg of PCR products was sequenced using the dye terminator DNA sequencing kit (Applied Biosystems, Japan) with 3.2 pmol of each primer (ORFI03$^+$, ORFI02$^-$) in an automatic sequencer (377 DNA Sequencer, Applied Biosystems).

Restriction fragment length polymorphism analysis of HTLV-I tax

Subgroup analysis of the Japanese HTLV-I *tax* genes was performed as described elsewhere.[8] Substitution at nucleotide position 8344 of the *tax* gene creates an AccII restriction site. One microliter of the first PCR product of the *tax* gene amplified with primers PXO1$^+$ and PXO2$^-$ was subjected to a further 20 cycles of PCR with primers PXI3$^+$ and PXI3$^-$. Two microliters of the nested PCR product was digested with 5 U of *Acc*II (Takara, Japan) in a 10 μl reaction volume at 37°C for 1 hr and the product was electrophoresed on a 1% agarose gel. When the PCR product was cut by *Acc*II, the sample was identified as *tax* A, and when uncut, the sample was identified as *tax* B.

Proviral load measurement

The HTLV-I provirus load in PBMC was measured in HAM/TSP patients and ACs as described.[27] A quantitative PCR reaction was performed using the ABI PRISM 7700 sequence detector (Perkin-Elmer Applied Biosystems). The amount of HTLV-I proviral DNA was calculated as follows: copy number of HTLV-1 (*tax*) per 10^4 PBMC = [copy number of *tax*/(copy number of β-actin/2)] $\times$ 10^4. The lower limit of detection was 1 copy per 10^4 PBMC.

RESULTS

Existence of p12K variant at low frequency in HAM/TSP patients

We analyzed 231 samples from 144 HAM/TSP patients, 41 ATL patients, and 46 ACs, all of them residing in Kagoshima, southern Japan. The grand consensus sequence of these 231 samples differed from the reference ATK strain at nucleotide position 6906 (A to G; leading to the amino acid change from serine in ATK to glycine in the grand consensus sequence), 6984 and 6985 (G to A in both positions; leading to the amino acid change from glycine in ATK to asparagine in the grand consensus sequence). There were HTLV-I subgroup-specific nucleotides at nucleotide positions 6900 and 6905. The nucleotide at position 6900 was T and the corresponding amino acid was serine in all of the HTLV-I sequences with *tax* A (31 cases in this study); this nucleotide was C and the amino acid was proline in all of the HTLV-I with *tax* B (200 cases in this study). The nucleotide at position 6905 was G in all HTLV-I sequences with *tax* A (31 cases in this study); in *tax* B this nucleotide was T but this difference does not correspond to an amino acid alteration. In Figure 1, we summarize the observed nucleotide alterations and amino acid changes that were not specific to an HTLV-I subgroup. In Table 1, we summarize amino acid changes that may influence the function of $p12^I$. The p12K variant was observed only in HAM/TSP patients; however, it was present at a low frequency (2 out of 144; 1.39%). All other samples, including HAM/TSP, ATL, and AC's had the p12R variant. One of the p12K subjects was a 65-year-old female who had had HAM/TSP for 8 years; the other was a 72-year-old female who had had HAM/TSP for 22 years. In each of these subjects, the *tax* subgroup was *tax* B. Serum anti-HTLV-I antibody titer and HTLV-I provirus load are summarized in Table 2. The HTLV-I provirus load tended to be lower in these two subjects, although a meaningful statistical analysis was not applicable because of the small number.

Premature stop codon preceding the p12R/K allele, alteration of initiation codon in p12 and other alteration

Interestingly, in 7 out of 144 HAM/TSP patients, a nucleotide substitution from G to A at nt positions 7087 (one patient) or 7088 (six patients) created a premature stop codon just upstream of the p12R/K allele (amino acid at position 87 of the $p12^I$ protein was changed from W to Stop). In another HAM/TSP patient, a nucleotide substitution from G to A at nt position 7078 also created a premature stop codon five amino acids upstream of the p12R/K allele (amino acid at position 82 of the p12 protein was changed from W to Stop). In one other HAM/TSP patient, nucleotide substitutions from T to C at nt 7086 and from G to A at nt 7088 were observed simultaneously, resulting in an amino acid substitution from W to R, one amino acid upstream of the p12R/K allele. In one other HAM/TSP patient, a nucleotide substitution from G to A at nt position 6836 destroyed the initiation codon of p12 (M to I). In ATL cases, there were two patients with a premature stop codon just upstream of the p12R/K allele out of 41 patients. However, in ACs, there was no subject with a premature stop codon in the *p12* gene. Ages and other laboratory findings are summarized in Table 2. There was an ATL specific nucleotide alteration at nt position 6909 in 3 out of 41 ATL patients (Fig. 1B), which was the most frequently observed alteration. The nucleotide alteration from G to A at this position changed the amino acid from aspartate to asparagine.

HTLV-I subgroup-specific nucleotide alteration, p12R/K allele, and the premature stop codon in p12 are stable over time (Table 3)

To examine if subgroup-specific nucleotide alterations, the p12R/K allele, and the premature stop codon were stable over time, we sequenced the HTLV-I p12 gene at different time points in cases with these nucleotide alterations. The nucleotide at position 6900 was T in HTLV-I sequences with *tax* A and this residue was C in HTLV-I with *tax* B. The nucleotide at position 6905 was G in HTLV-I sequences with *tax* A and this residue was T in HTLV-I with *tax* B. These nucleotide alterations existed stably for 7 years in the HAM 70 case (Table 3). The p12R allele existed stably for 7 years in the HAM 57 case. Also, the p12K allele existed stably for 9 years in the HAM 79 case (Table 3). The premature stop codon in the *p12* gene was also stably maintained in HAM 105 and in HAM 181 for 9 years in both cases (Table 3). No case was found in which these sequence variants changed over time in one individual.

HTLV-I with premature stop codon in p12 gene is transmissible (Table 4)

To examine whether HTLV-I with a premature stop codon in the *p12* gene is transmissible, we sequenced the *p12* gene in asymptomatic carriers who are family members of cases with a premature stop codon in the *p12* gene. HTLV-I carriers who are family members of three HAM/TSP patients with a *p12* premature stop codon were examined. Each family member had a sequence of the *p12* gene that was identical to that of the HAM/TSP patients in their respective family. For example, the husband of HAM 181 had an identical *p12* sequence with substitution at 7078, which created a stop codon that was observed only in this family. The wife of HAM 201 had an identical *p12* gene sequence with substitutions at 6840, 7094 (creating a stop codon), and 7134, in addition to the HTLV-I subgroup-specific substitutions at 6900 and 6905. A sister and the mother of HAM 790 had an identical *p12* gene sequence with the stop codon at nucleotide 7094.

HTLV-I with destroyed initiation codon in the p12 gene was also transmitted (Table 4)

To examine whether HTLV-I with a destroyed initiation codon in the *p12* gene was also transmitted, we checked family members of patient HAM 271 who carried an HTLV-I provirus with a destroyed initiation codon. Samples from two sisters of this patient were available, one of whom was previously diagnosed as HAM/TSP. The p12 sequence was identical, with a destroyed initiation codon of *p12*, among these three sisters.

DISCUSSION

Recently, the function of the $p12^I$ of HTLV-I has been under debate, and natural variants of *p12* at position 88 (arginine,

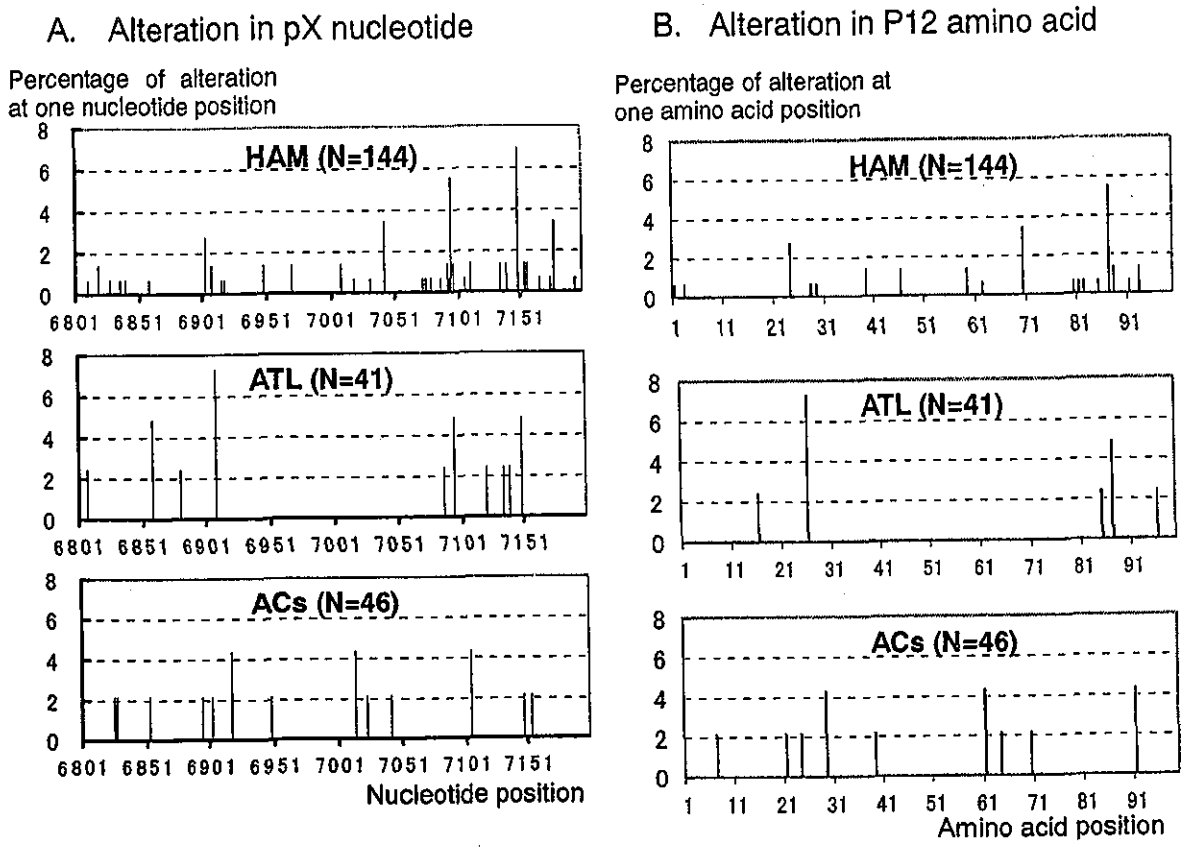

FIG. 1. Summary of the nucleotide and amino acid alterations. (A) Summary of the nucleotide alterations in pX that covers the p12[I] protein. Upper column: HAM/TSP patients. Middle column: ATL patients. Lower column: Asymptomatic carriers. *x*-axis, nucleotide position. *y*-axis, percentage of nucleotide alteration at one nucleotide position. (B) Summary of the amino acid alterations in the p12[I] protein. Upper column: HAM/TSP patients. Middle column: ATL patients. Lower column: Asymptomatic carriers. *x*-axis, amino acid position of the p12[I] protein. *Y*-axis, percentage of the amino acid alteration at one amino acid position.

p12R and lysine, p12K) were reported.[21] Lysine at position 88 in p12[I] is a ubiquitylation site and a shorter life of p12K compared to p12R was reported. p12K was previously reported to be frequent and specific in HAM/TSP patients,[21] but there was also a conflicting report.[22] The main purpose of the present study was to elucidate if variations in the *p12* gene were associated with HTLV-I related diseases, especially with respect to the distribution of p12 R/K variation in HAM/TSP, ATL, and ACs. We also examined whether the p12R/K variation was associated with the HTLV-I *tax* viral genotype, which we previously reported to influence the risk of HAM/TSP development.[8]

The p12K variant was observed in only two HAM/TSP pa-

TABLE 1. SUMMARY OF AMINO ACID CHANGES IN p12[I] PROTEIN THAT MAY INFLUENCE THE FUNCTION[a]

Amino acid position (change in amino acid)	*HAM/TSP (N = 144)*	*ATL (N = 41)*	*ACs (N = 46)*
1 (M to I)	1 (0.7%)	0	0
82 (W to Stop)	1 (0.7%)	0	0
87 (W to Stop)	7 (4.9%)	2 (4.9%)	0
88 (R to K)	2 (1.4%)	0	0
Total	11 (7.6%)	2 (4.9%)	0

[a]Number of cases that have amino acid change at the position described in the left column is stated. Amino acid change of p12[I] is shown in parentheses in the left column. Percentage of cases are shown in parentheses in the HAM/TSP, ATL, and ACs columns.

TABLE 2. CHARACTERIZATION OF HAM/TSP PATIENTS WITH DESTROYED INITIATION CODON, PREMATURE STOP CODON, AND p12R/K ALLELE IN THE p12 GENE

Amino acid position (change in amino acid)	*No. of cases*	*Age*	*Anti-HTLV-I antibody[a] (PA)*	*HTLV-I provirus load[a]*
1 (M to I)	1	43	8192	1954
82 (W to Stop)	1	63	32768	1343
87 (W to Stop)	7	41[b]	8192	641
88 (R to K)	2	69[b]	9216	146
All HAM/TSP patients	144	56[b]	8192	586

[a]Anti-HTLV-I antibody titer and HTLV-I provirus load are stated as median value.
[b]Mean age is shown.

tients but did not occur either in ATL patients or in ACs. However, the frequency of p12K was very low (2 out of 144; 1.4%). Regarding the association of p12R/K alleles and the *tax* subgroup, two HTLV-I-seropositive subjects with p12K were classified to have *tax* B. However, another HTLV-I-seropositive individual with *tax* B (119 HAM patients) had p12R. Also, of the 142 HAM/TSP patients who carried p12R, 23 HAM/TSP patients had *tax* A and 119 had *tax* B. Trovato also reported that p12R/K alleles were found regardless of the geographical origin.[21] These findings suggest that the p12R/K variation is not specifically associated with the HTLV-I subgroup. Also, the very low frequency of the p12K variant observed among HAM/TSP patients in Japan cannot be explained by the particular distribution of the HTLV-I subgroup in Japan: most of the HTLV-I in Japan belongs to Cosmopolitan B, while Cosmopolitan A is widely distributed through the world.

Although the p12K variant, which may have a decreased biological effect because of its shorter life, was found at a very low frequency in HAM/TSP patients, other variations in the *p12* gene that can affect the function of *p12* were found in HAM/TSP and in ATL patients. A premature stop codon was found in eight HAM/TSP patients and in two ATL patients but not in ACs. Trovato *et al.*[21] also reported this termination codon immediately preceding the lysine in one ATL patient who also had HAM/TSP. Because the $p12^{I}$ sequence with a premature stop codon immediately preceding the p12R/K allele had arginine in our study, and the p12R/K allele was lysine in Trovato's study, this stop codon does not appear to be associated with the p12R/K variation. Regarding the association with the termination codon immediately preceding the p12R/K variation and the *tax* subgroup, there were six HAM/TSP patients with *tax* B and one HAM/TSP patient with *tax* A. Thus, this termination codon immediately preceding the p12R/K variation was also not specifically associated with the *tax* subgroup.

To test whether HTLV-I having a *p12* sequence with either arginine (p12R) or lysine (p12K) at position 88 and HTLV-I with truncated $p12^{I}$ could persist stably over time, we compared the HTLV-I *p12* sequences at different time points. The observed *p12* nucleotide substitutions were the same in each person on each occasion (Table 3), suggesting that neither p12R/K nor a premature stop codon in $p12^{I}$ influences the course of HTLV-I infection. To examine whether HTLV-I with such a truncated $p12^{I}$ was transmissible, we further compared the *p12* sequence between HAM/TSP patients with a termination codon

TABLE 3. COMPARISON OF HTLV-I *p12* SEQUENCES AT DIFFERENT TIME POINTS WITH THE GRAND CONSENSUS SEQUENCE[a]

		Nucleotide change at position (amino acid position)					
	Date	*6900 (23)*	*6905 (24)*	*7078 (82)*	*7086 (85)*	*7093 (87)*	*7096 (88)*
Consensus		C (P)	T (P)	G (W)	C (L)	G (W)	G (R)
HAM 57	July 4, 1990				T (F)		G (R)
	August 29, 1997				T (F)		G (R)
HAM 70	June 27, 1990	T (S)	G (S)				G (R)
	February 27, 1998	T (S)	G (S)				G (R)
HAM 79	April 17, 1991						A (K)
	October 11, 2000						A (K)
HAM 105	March 11, 1992					A (Stop)	G (R)
	July 12, 2001					A (Stop)	G (R)
HAM 181	March 27, 1991			A (Stop)			G (R)
	January 15, 2000			A (Stop)			G (R)

[a]Amino acid of $p12^{I}$ is shown in parentheses.

TABLE 4. COMPARISON OF HTLV-I *p12* SEQUENCES WITHIN PEDIGREE WITH THE GRAND CONSENSUS SEQUENCE[a]

		Nucleotide change at position (amino acid change at position)						
	Sex	*6836 (1)*	*6840 (3)*	*6900 (23)*	*6905 (24)*	*7078 (82)*	*7094 (87)*	*7134*
Consensus		G (M)	T (L)	C (P)	T (P)	G (W)	G (W)	G
HAM 181	F					A (Stop)		
Husband of HAM 181	M					A (Stop)		
HAM 201	M		C (L)	T (S)	G (S)		A (Stop)	C
Wife of HAM 201	F		C (L)	T (S)	G (S)		A (Stop)	C
HAM 790	F						A (Stop)	
Sister of HAM 790	F						A (Stop)	
Mother of HAM 790	F						A (Stop)	
HAM 271	F	A (I)						
Sister of HAM 271 (AC)	F	A (I)						
Sister of HAM 271 (HAM)	F	A (I)						

[a]In the HAM 271 family, one sister was an asymptomatic HTLV-I carrier [HAM 271 (AC)] and one other sister was an HAM/TSP patient [HAM 271 (HAM)]. These three cases had an identical *p12* sequence with a destroyed initiation codon in the *p12* gene. Amino acid of $p12^I$ is shown in parentheses.

in the *p12* gene and their family members infected with HTLV-I. Interestingly, the *p12* sequences with a premature stop codon at either position 82 and 87 in HAM/TSP patients were identical in asymptomatic family members of HAM/TSP patients in each family. These findings also suggest that truncations of $p12^I$ at position 82 or 87 do not influence the infectivity of HTLV-I, although it was possible that the truncated $p12^I$ retained its function. However, in our study there was an HAM/TSP patient (HAM 271) with $p12^I$ in whom the $p12^I$ initiation codon was destroyed. In this case, the nucleotide at position 6836 had a substitution from G to A, changing the initiation codon ATG to ATA. We were interested to determine whether such a p12 with a destroyed initiation codon was transmissible in the patient's family. We examined HTLV-I sequences from two other HTLV-I-infected sisters in this family. One of the sisters was an HAM/TSP patient, while the other was an AC. The *p12* sequences were identical among these three sisters, with the same substitution at nt 6836 (G → A) that destroyed the initiation codon of *p12*. This observation indicates that the destroyed *p12* was not a *de novo* mutation that happened in patient HAM 271, but rather was transmitted from their mother to the three sisters in this family. This contrasts with the observation that a putative immune escape mutation in the *tax* gene was observed in an ATL patient but not in the respective consensus sequence of asymptomatic HTLV-I carriers in the same family.[28] These findings strongly suggest that HTLV-I $p12^I$ is dispensable for HTLV-I transmission and the maintenance of HTLV-I infection. Regarding the relation between sequence variations in the HTLV-I *p12* gene and their association with HTLV-I-related diseases, lysine at position 88 (p12K) itself was not frequently observed in HAM/TSP patients (2 out of 144 HAM/TSP patients; 1.4%). However, the p12K variant, premature stop codons, and the destruction of the initiation codon were observed in 11 patients out of 144 HAM/TSP patients (7.4%), whereas none of these variations was observed in ACs. These variations in the *p12* gene may reduce the function of $p12^I$. Because p12K has a shorter life compared to p12R, and a premature stop codon in the $p12^I$ may reduce its function, the destruction of the initiation codon in the *p12* gene presumably ablates the function of $p12^I$. At the beginning of this study, we expected that alterations that reduce the function of the $p12^I$ would be less frequent in HAM/TSP, because HAM/TSP patients usually have a higher provirus load than ACs, and $p12^I$ had been suggested to confer a proliferative effect on HTLV-I-infected cells in an *in vitro* study. It is possible that the effects of $p12^I$ *in vivo* differ from its effects *in vitro*. However, the observed difference between HAM/TSP patients and ACs in the prevalence of these alterations that may reduce the function of $p12^I$ did not reach statistical significance, and it is therefore premature to conclude that mutations of the *p12* gene are implicated in the pathogenesis of HTLV-I-associated diseases. Further study with a larger number of ACs is necessary to clarify this point.

SEQUENCE DATA

DDBJ accession numbers: The accession numbers of the pX sequence including the entire *p12* gene in HAM/TSP cases are successively from AB127436 through AB127579. The accession numbers of the pX sequence including the entire *p12* gene in ATL cases are successively from AB154777 through AB154817. The accession numbers of the pX sequence including the entire *p12* gene in ACs are successively from AB158146 through AB158191. The accession numbers of the pX sequence including the entire *p12* gene at different occasions in Table 3 are AB127439 for HAM 57 at July 4, 1990, AB158267 for HAM 57 at August 29, 1997, AB127442 for HAM 70 at June 27, 1990, AB158266 for HAM 70 at February 27, 1998, AB127447 for HAM 79 at April 17, 1991,

AB158268 for HAM 79 at October 11, 2000, AB127458 for HAM 105 at March 11, 1992 and AB158270 for HAM 105 at July 12, 2001, AB127485 for HAM 181 at March 27, 1991 and AB158269 for HAM 181 at January 15, 2000. The accession numbers of the pX sequence including the entire *p12* gene of HAM/TSP patients and family members in Table 4 are AB127485 for HAM 181, AB158271 for the husband of HAM 181, AB127493 for HAM 201, AB158272 for the wife of HAM 201, AB127521 for HAM 271, AB158275 for the asymptomatic sister of HAM 271, AB158276 for the HAM/TSP sister of HAM 271, AB127562 for HAM 790, AB158273 for the sister of HAM 790, and AB158274 for the mother of HAM 790.

ACKNOWLEDGMENTS

This study was supported by in part from Takeda Science Foundation. We thank Ms. T. Muramoto and Ms. Y. Nishino (Department of Neurology and Geriatrics, Kagoshima University, Japan) for their excellent technical assistance. We also thank Professor Charles R.M. Bangham (*Immunology* Department, Imperial College Faculty of Medicine, United Kingdom) for critical reading of the manuscript. Presented in part at the 45th Conference Annual Meeting of the Japanese Society of Haematology, Nagoya, Japan, 29–31 August 2003. Informed consent was obtained from all HTLV-I carriers and patients. This research was approved by the institutional review boards of the author's institutions, and human experimentation guidelines of the U.S. Development of Health and Human Services and those of the author's institutions were followed in the conduct of clinical research. The authors have no commercial or other associations that might pose a conflict of interest.

REFERENCES

1. Poiesz BJ, Ruscetti FW, Gazdar AF, Bunn PA, Minna JD, and Gallo RC: Detection and isolation of type C retrovirus particles from fresh and cultured lymphocytes of a patient with cutaneous T-cell lymphoma. Proc Natl Acad Sci USA 1980;77:7415–7419.
2. Yoshida M, Miyoshi I, and Hinuma Y: Isolation and characterization of retrovirus from cell lines of human adult T-cell leukemia and its implication in the disease. Proc Natl Acad Sci USA 1982;79:2031–2035.
3. Gessain A, Barin F, Vernant JC, *et al.*: Antibodies to human T-lymphotropic virus type-I in patients with tropical spastic paraparesis. Lancet 1985;2:407–410.
4. Osame M, Usuku K, Izumo S, *et al.*: HTLV-I associated myelopathy, a new clinical entity. Lancet 1986;1:1031–1032.
5. Tajima K: The 4th nation-wide study of adult T-cell leukemia/lymphoma (ATL) in Japan: *Estimates of risk of ATL and its geographical and clinical features.* The T- and B-cell Malignancy Study Group. Int J Cancer 1990;45:237–243.
6. Kaplan JE, Osame M, Kubota H, *et al.*: The risk of development of HTLV-I-associated myelopathy/tropical spastic paraparesis among persons infected with HTLV-I. J Acquir Immune Defic Syndr 1990;3:1096–1101.
7. Daenke S, Nightingale S, Cruickshank JK, and Bangham CR: Sequence variants of human T-cell lymphotropic virus type I from patients with tropical spastic paraparesis and adult T-cell leukemia do not distinguish neurological from leukemic isolates. J Virol 1990;64:1278–1282.
8. Furukawa Y, Yamashita M, Usuku K, Izumo S, Nakagawa M, and Osame M: Phylogenetic subgroups of human T cell lymphotropic virus (HTLV) type I in the tax gene and their association with different risks for HTLV-I-associated myelopathy/tropical spastic paraparesis. *J Infect Dis 2000;182:1343–1349*
9. Giebler HA, Loring JE, van Orden K, *et al.*: Anchoring of CREB binding protein to the human T-cell leukemia virus type 1 promoter: A molecular mechanism of Tax transactivation. Mol Cell Biol 1997;17:5156–5164.
10. Siekevitz M, Feinberg MB, Holbrook N, Wong-Staal F, and Greene WC: *Activation of interleukin 2 and interleukin* 2 receptor (Tac) promoter expression by the trans-activator (tat) gene product of human T-cell leukemia virus, type I. Proc Natl Acad Sci USA 1987;84:5389–5393.
11. Brown DA, Nelson FB, Reinherz EL, and Diamond DJ: The human interferon-gamma gene contains an inducible promoter that *can* be transactivated by tax I and II. Eur J Immunol 1991;21: 1879–1885.
12. Fujii M, Sassone-Corsi P, and Verma IM: c-fos promoter trans-activation by the tax1 protein of human T-cell leukemia virus type I. Proc Natl Acad Sci USA 1988;85:8526–8530.
13. Berneman ZN, Gartenhaus RB, Reitz MS Jr, *et al.*: Expression of alternatively spliced human T-lymphotropic virus type I pX mRNA in infected cell lines and in primary uncultured cells from patients with adult T-cell leukemia/lymphoma and healthy carriers. Proc Natl Acad Sci USA 1992;89:3005–3009.
14. Franchini G, Mulloy JC, Koralnik IJ, *et al.*: The human T-cell leukemia/lymphotropic virus type I p12I protein cooperates with the E5 oncoprotein of bovine papillomavirus in cell transformation and binds the 16-kilodalton subunit of the vacuolar *H+ ATPase.* J Virol 1993;67:7701–7704.
15. Mulloy JC, Crownley RW, Fullen J, Leonard WJ, and Franchini G: The human T-cell leukemia/lymphotropic virus type I p12I proteins bind the interleukin-2 receptor beta and gammac chains and affects their expression on the cell surface. J Virol 1996; 70:3599–3605.
16. Collins ND, Newbound GC, Albrecht B, Beard JL, Ratner L, and Lairmore MD: Selective ablation of human T-cell lymphotropic virus type 1 p12I reduces viral infectivity in vivo. Blood 1998;91:4701–4707.
17. Koralnik IJ, Fullen J, and Franchini G: The p12I, p13II, and p30II proteins encoded by human T-cell leukemia/lymphotropic virus type I open reading frames I and II are localized in three different cellular compartments. J Virol 1993;67:2360–2366.
18. Ding W, Albrecht B, Kelley RE, *et al.*: Human T-cell lymphotropic virus type I p12(I) expression increases cytoplasmic calcium to enhance the activation of nuclear factor of activated T cells. J Virol 2002;76:10374–10382.
19. *Johnson JM, Nicot C, Fullen J, et al.: Free major* histocompatibility complex class I heavy chain is preferentially targeted for degradation by human T-cell leukemia/lymphotropic virus type 1 p12(I) protein. J Virol 2001;75:6086–6094.
20. Nicot C, Mulloy JC, Ferrari MG, *et al.*: HTLV-1 p12(I) protein enhances STAT5 activation and decreases the interleukin-2 requirement for proliferation of primary human peripheral blood mononuclear cells. Blood 2001;98:823–829.
21. Trovato R, Mulloy JC, Johnson JM, Takemoto S, de Oliveira MP, and Franchini G: A lysine-to-arginine change found in natural alleles of the human T-cell lymphotropic/leukemia virus type 1 p12(I) protein greatly influences its stability. J Virol 1999;73:6460–6467.
22. Martins ML, Soares BC, Ribas JG, *et al.*: Frequency of p12K and p12R alleles of HTLV type 1 in HAM/TSP patients and in asymptomatic HTLV type 1 carriers. AIDS Res Hum Retroviruses 2002;18:899–902.
23. Osame M: HTLV. In: *Human Retrovirology* (Blattner W, ed.). Raven, New York, 1990, pp. 191–197.

24. Shimoyama M: Diagnostic criteria and classification of clinical subtypes of adult T-cell leukaemia-lymphoma. A report from the Lymphoma Study Group (1984–87). Br J Haematol 1991;79:428–437.
25. Furukawa Y, Kubota R, Eiraku N *et al.*: Human T-cell lymphotropic virus type I (HTLV-I) related clinical and laboratory findings in HTLV-I infected blood donors. J Acquir Immune Defic Syndr 2003;32:328–334.
26. Seiki M, Hattori S, Hirayama Y, and Yoshida M: Human adult T-cell leukemia virus: Complete nucleotide sequence of the provirus genome integrated in leukemia cell DNA. Proc Natl Acad Sci USA 1983; 80:3618–3622.
27. Nagai M, Usuku K, Matsumoto W, *et al.*: Analysis of HTLV-I proviral load in 202 HAM/TSP patients and 243 asymptomatic HTLV-I carriers: High proviral load strongly predisposes to HAM/TSP. J Neurovirol 1998;4:586–593.
28. Furukawa Y, Kubota R, Tara M, Izumo S, and Osame M: Existence of escape mutant in HTLV-I tax during the development of adult T-cell leukemia. Blood 2001;97:987–993.

Address reprint requests to:
Yoshitaka Furukawa
Division of Blood Transfusion Medicine
Kagoshima University Hospital
8-35-1 Sakuragaoka
Kagoshima 890-8520, Japan

E-mail: furukawy@m2.kufm.kagoshima-u.ac.jp

Available online at www.sciencedirect.com
SCIENCE DIRECT®
Tetrahedron Letters
Tetrahedron Letters 45 (2004) 3651–3654

A new polymer-supported Evans-type chiral auxiliary derived from α-hydroxy-β-amino acid, phenylnorstatine: synthesis and application in solid-phase asymmetric alkylation reactions

Tomoya Kotake, S. Rajesh, Yoshio Hayashi, Yoshie Mukai, Mitsuhiro Ueda, Tooru Kimura and Yoshiaki Kiso*

Department of Medicinal Chemistry, Center for Frontier Research in Medicinal Science, Kyoto Pharmaceutical University, Yamashina-ku, Kyoto 607-8412, Japan

Received 6 February 2004; revised 2 March 2004; accepted 5 March 2004

Abstract—Based on a new anchoring strategy, a polymer-supported chiral oxazolidinone was prepared starting from (2*R*,3*S*)-3-amino-2-hydroxy-4-phenylbutanoic acid (phenylnorstatine, Pns) and Wang resin. Solid-phase asymmetric alkylation on this resin proceeded in high diastereoselectivity comparable to that of conventional solution-phase model experiments. This study suggests that anchoring through the 5-position of oxazolidinone is highly suited to achieving diastereoselective alkylation reactions on solid-support.

Recently, solid-phase organic synthesis has become a popular methodology for the preparation of organic molecules,[1] especially the preparation of compound libraries in the process of drug discovery.[2] It allows for a facile isolation of the desired compounds with easy elimination of by-products and excess reagents using a full- or semi-automatic process. Polymer-supported chiral auxiliaries are especially advantageous because they can be recovered by simple filtration and potentially recycled. Evans' oxazolidinone is one of the most versatile chiral auxiliaries for asymmetric acyl group-based transformation.[3] The attachment of Evans' oxazolidinone to solid-supports and its utility in asymmetric alkylation,[4] aldol condensation,[5] and Diels–Alder,[6] and 1,3-dipolar[7] cycloadditions have been reported using **1** (Fig. 1A). However, the application of **1** is limited, probably due to the difficulty of monitoring and optimizing the solid-phase reaction more than the corresponding solution-phase reactions. In addition, the solid-phase asymmetric alkylation on the resin **1** has not been accomplished in a high stereoselective manner (max 90% ee) and a marked undesired effect of the solid-supports on the yield and ee was reported.[4] One reason for these undesired results could be that the critical chiral discriminating unit, that is, the benzyl group at

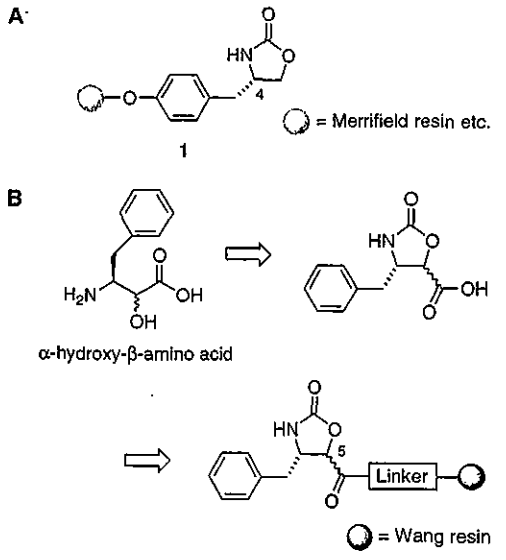

Figure 1. Polymer-supported Evans-type chiral auxiliaries. (A) Chiral auxiliary anchored at the 4-position.[4-7] (B) The new auxiliary derived from α-hydroxy-β-amino acid anchored at the 5-position.

Keywords: Evans' oxazolidinone; Chiral auxiliary; Phenylnorstatine; Asymmetric alkylation; Solid-phase; Polymer-supported.
* Corresponding author. Tel.: +81-75-595-4635; fax: +81-75-591-9900; e-mail: kiso@mb.kyoto-phu.ac.jp

0040-4039/$ - see front matter © 2004 Elsevier Ltd. All rights reserved.
doi:10.1016/j.tetlet.2004.03.043

the 4-position of the oxazolidinone ring in **1**, was used to anchor the solid-support.

Hence, to create a new anchor liberating the benzyl group, we focused on the chiral α-hydroxy-β-amino acids, phenylnorstatine [Pns, (2*R*,3*S*)-3-amino-2-hydroxy-4-phenylbutanoic acid] and its (2*S*,3*S*)-stereoisomer, allophenylnorstatine (Apns), which are well-known units with the hydroxymethylcarbonyl (HMC) isostere necessary for inhibiting aspartyl proteases.[8] As shown in Figure 1B, these α-hydroxy-β-amino acids can be converted to the corresponding oxazolidinones with a carboxyl group at the 5-position of the ring for anchoring to the solid-support. Here, we describe the synthesis of a new polymer-supported Evans' chiral auxiliary derived from Pns and demonstrate that solid-phase asymmetric alkylation proceeds with high stereoselectivity parallel to that obtained with the model substrate under classical solution conditions.

In the design of new polymer-supported oxazolidinone, piperidine-4-carboxylic acid was used as a linker, which can connect the chiral auxiliary through a base-insensitive tertiary-amide bond. Wang resin[9] was used as the solid-support, since the ester bond between the linker and resin can be easily formed by standard condensation methods and cleaved by mild acids like TFA or methanolysis to monitor the reaction.

The synthesis of oxazolidinone derivative **4** is outlined below (Scheme 1). Boc—Pns—OH[10] **2** was coupled to benzyl piperidine-4-carboxylate·HCl by the EDC–HOBt method[11] to give **3**. Removal of the *N*-Boc group of **3** and subsequent reaction with 1,1′-carbonyldiimidazole (CDI)[12] gave the desired oxazolidinone **4** in good yields.[13] During this cyclization reaction, no epimerization at the 5-position, and no aziridine by-product formation[14] were observed. Oxazolidinone **4** was then *N*-3-phenylpropionylated and the resultant carboximide **5a** was subjected to a model alkylation study in the solution-phase.[15] As Table 1 shows, the new oxazolidinone derivative **4** could function as an efficient chiral auxiliary with suitable reactivity in terms of yield and stereoselectivity. In addition, no disruption of both the oxazolidinone ring and the benzyl ester was observed during the cleavage with LiOOH.[16] Similar results were also obtained in the use of other imides **5b** and **5c** with *N*-phenoxyacetyl and *N*-propionyl groups, respectively (Table 1).

In the case of *N*-acyloxazolidinone derived from Boc—Apns—OH, epimerization at the 5-position was observed during the base treatment, suggesting that the 5-position as well as the desired α-position of the acyl group were deprotonated by LDA, while deprotonation in the Pns-derived *N*-acyloxazolidinone was specific to the α-position. This was probably due to increased acidity at

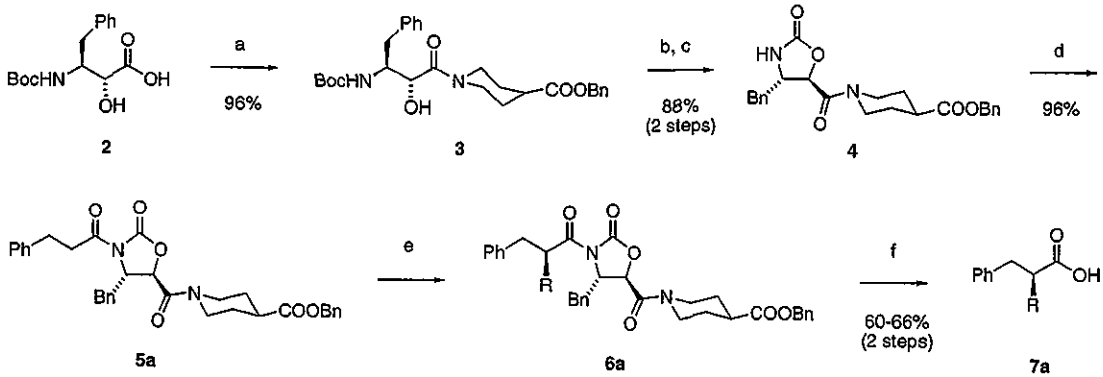

Scheme 1. Reagents and conditions: (a) benzyl piperidine-4-carboxylate·HCl, HOBt·H_2O, EDC·HCl, Et_3N, DMF, 0 °C to rt; (b) 4 M HCl/1,4-dioxane, 0 °C to rt; (c) Et_3N, CDI, THF, 0 °C to rt; (d) 3-phenylpropionic acid, ^{t}BuCOCl, Et_3N, LiCl, THF, −18 °C to rt; (e) LDA, RX, THF, −78 to 0 °C; (f) LiOH, 30% H_2O_2, THF–H_2O (3:1), 0 °C.

Table 1. Results of asymmetric alkylation

Entry	Imide	R^2X	Solid-phase		Solution-phase	
			Yield (%)[a]	Ee (%)[b]	Yield (%)[c]	Ee (%)[b]
1	**10/5a**	MeI	48	85	62	86
2	**10/5a**		54	96	66	96
3	**10/5a**		51	94	64	95
4	**10/5a**		47	92	60	90
5	**11/5b**		38	96	48	96
6	**12/5c**	BnBr	40	97	57	98

[a] Yield in four steps based on original loading of Wang resin (see Scheme 2).
[b] Determined by HPLC analysis after conversion to the corresponding (*S*)-phenylethyl amide derivatives.
[c] Yield in two steps starting from **5** (see Scheme 1).

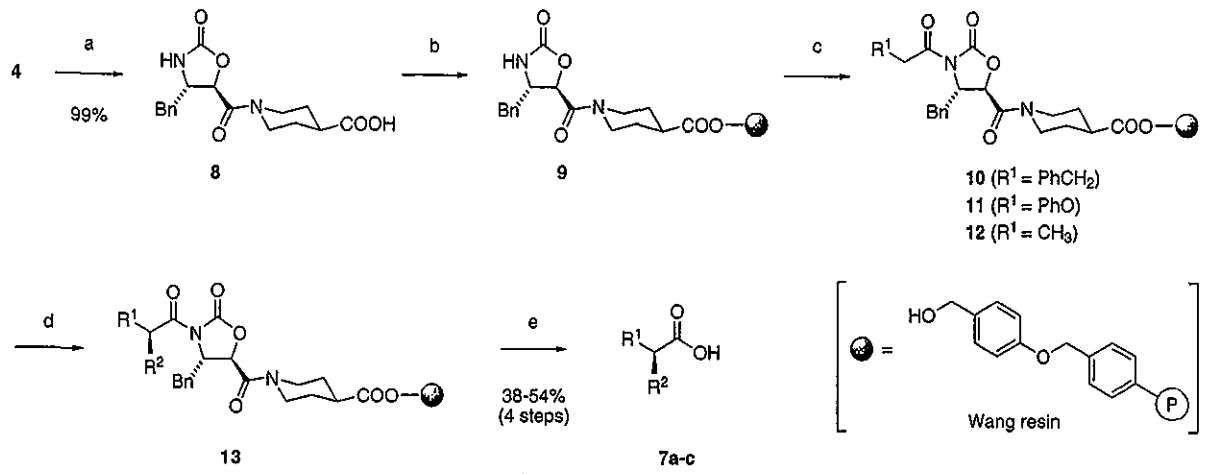

Scheme 2. Reagents and conditions: (a) H_2, Pd/C, MeOH–H_2O (9:1), rt, overnight; (b) Wang resin, DIC, DMAP, DMF, rt, 3 h; (c) $R^1CH_2CO_2H$, 2-chloro-1-methylpyridinium iodide, Et_3N, DMAP, CH_2Cl_2, rt, 2 h; (d) LDA, R^2X, THF, 0 °C, 3.5 h; (e) LiOH, 30% H_2O_2, THF–H_2O (3:1), 0 °C, 1 h.

the 5-position of the Apns-derived oxazolidinone caused by steric repulsion between the benzyl and carboxamide groups in a *cis*-configuration.

Hence, for the solid-phase synthesis, Pns-derived oxazolidinone **4** was selected and its benzyl ester was removed by hydrogenolysis, and the resultant carboxylic acid **8** was attached to the Wang resin by the established method with 1,3-diisopropylcarbodiimide (DIC)[17] in the presence of a catalytic amount of DMAP (Scheme 2). Analysis of the loading rate by methanolysis of the resin **9** gave a complete recovery of the corresponding methyl ester, indicating that quantitative loading was achieved. It is pertinent to note that the previous reported auxiliary **1** on Wang resin having only 56% of loading might have potential side reactions by the residual free-hydroxyl group.[4] On the contrary, we were able to efficiently synthesize a new Wang resin-supported Evans-type chiral auxiliary **9** with a quantitative loading.

For the solid-phase asymmetric alkylation, to a well-swollen carboximide resin **10–12** in THF, derived from **9** by the mixed anhydride-LiCl N-acylation[18] or Mukaiyama reagent,[19] was added LDA (2 equiv) at 0 °C, followed by the addition of alkyl halide (10 equiv). After stirring for 3 h at the same temperature, the solid-phase reaction was quenched by adding saturated aqueous NH_4Cl. The resin was recovered by filtration and was subsequently washed with THF and MeOH to give **13**. LiOOH-mediated chemoselective hydrolysis of **13** gave the desired chiral α-alkylated carboxylic acids **7a–c**.[20] Since no disruption of the ester bond between the linker and resin was observed during these steps and methanolysis of recovered resin afforded the corresponding oxazolidinone methyl ester in high yield (94% yield Table 1, entry 2), it indicated that the polymer-supported auxiliary was stable to LiOOH treatment. Therefore, it is considered that the recovered resin **9** has a potential for reuse. Enantiomeric excess of the obtained acids was determined by HPLC analysis after derivatization to the corresponding (*S*)-phenylethyl amides by the EDC–HOBt method. As Table 1 shows, high stereoselectivity (85–97% ee) comparable to the solution-phase model experiments was obtained in this solid-phase system with a total yield of 38–54% (in four steps), calculated from the original loading of Wang resin. These results suggest that anchoring to the resin at the 5-position of the oxazolidinone ring is highly suitable for realizing reasonable enantiomeric ratios, probably achieving greater freedom from the polystyrene scaffold than the previous auxiliary involving the 4-position. It also suggests that the asymmetric alkylation reaction proceeded through the same chelation controlled model as reported in standard Evans-type oxazolidinone chemistry.[3a] These findings would resolve the concern raised by Burgess and Lim[4] in the solid-phase asymmetric alkylation using the polymer-supported Evans' chiral auxiliary, and our new polymer-supported oxazolidinone is applicable in the synthesis of a variety of chiral α-alkylated carboxylic acids.

In conclusion, we have developed a new polymer-supported Evans-type chiral auxiliary, anchored to the Wang resin through a carboxyl group at the 5-position of the oxazolidinone ring and a piperidine-4-carboxyl linker, and found it to be a useful tool for solid-phase asymmetric alkylation with no reduction in stereoselectivity. This convenient polymer-supported chiral auxiliary is applicable in the preparation of a library of chiral α-branched carboxylic acids such as 3-phenylpropionic acid derivatives having inhibitory activity against serine proteases.[21] Further studies of well-known asymmetric reactions in the use of the Evans' auxiliary, such as aldol condensation and cycloadditions, and the recycling of the resin are under investigation.

Acknowledgements

This research was supported in part by grants and the Frontier Research Program of the Ministry of Education, Science and Culture of Japan.

References and notes

1. (a) Seneci, P. *Solid Phase and Combinatorial Technologies*; John Wiley & Sons: New York, 2000; (b) Obrecht, D.; Villalgordo, J. M. In *Solid-Supported Combinatorial and Parallel Synthesis of Small Molecular-Weight Compound Libraries. Tetrahedron Organic Chemistry Series*; Elsevier: Oxford, 1998; Vol. 17.
2. (a) Geysen, H. M.; Schoenen, F.; Wagner, D.; Wagner, R. *Nat. Rev. Drug Discovery* **2003**, *2*, 222–230; (b) Gallop, M. A.; Barrett, R. W.; Dower, W. J.; Fodor, S. P. A.; Gordon, E. M. *J. Med. Chem.* **1994**, *37*, 1233–1251.
3. (a) Evans, D. A. *Aldrichim. Acta* **1982**, *15*, 23–32; (b) Ager, D. J.; Prakash, I.; Schaad, D. R. *Aldrichim. Acta* **1997**, *30*, 3–11.
4. Burgess, K.; Lim, D. *Chem. Commun.* **1997**, 785–786.
5. (a) Purandare, A. V.; Natarajan, S. *Tetrahedron Lett.* **1997**, *38*, 8777–8780; (b) Phoon, C. W.; Abell, C. *Tetrahedron Lett.* **1998**, *39*, 2655–2658.
6. Winkler, J. D.; McCoull, W. *Tetrahedron Lett.* **1998**, *39*, 4935–4936.
7. (a) Faita, G.; Paio, A.; Quadrelli, P.; Rancati, F.; Seneci, P. *Tetrahedron Lett.* **2000**, *41*, 1265–1269; (b) Faita, G.; Paio, A.; Quadrelli, P.; Rancati, F.; Seneci, P. *Tetrahedron* **2001**, *57*, 8313–8322; (c) Desimoni, G.; Faita, G.; Galbiati, A.; Pasini, D.; Quadrelli, P.; Rancati, F. *Tetrahedron: Asymmetry* **2002**, *13*, 333–337.
8. (a) Mimoto, T.; Kato, R.; Takaku, H.; Nojima, S.; Terashima, K.; Misawa, S.; Fukazawa, T.; Ueno, T.; Sato, H.; Shintani, M.; Kiso, Y.; Hayashi, H. *J. Med. Chem.* **1999**, *42*, 1789–1802; (b) Mimoto, T.; Hattori, N.; Takaku, H.; Kisanuki, S.; Fukazawa, T.; Terashima, K.; Kato, R.; Nojima, S.; Misawa, S.; Ueno, T.; Imai, J.; Enomoto, H.; Tanaka, S.; Sakikawa, H.; Shintani, M.; Hayashi, H.; Kiso, Y. *Chem. Pharm. Bull.* **2000**, *48*, 1310–1326.
9. Wang resin was purchased from Watanabe Chem. Ind., Ltd (Hiroshima, Japan), loading 0.75 mmol/g, 100–200 mesh, polystyrene with 1% cross linking with divinylbenzene.
10. Boc—Pns—OH was prepared from H—Pns—OH, which was purchased from Nippon Kayaku (Tokyo, Japan).
11. König, W.; Geiger, R. *Chem. Ber.* **1970**, *103*, 788–798.
12. Bunnage, M. E.; Davies, S. G.; Goodwin, C. J.; Ichihara, O. *Tetrahedron* **1994**, *50*, 3975–3986.
13. Chemical data for benzyl *N*-[(4*S*)-benzyl-1,3-oxazolidin-2-one-5-carbonyl]piperidine-4-carboxylate (4): mp 91–93 °C; R_f 0.55 (*n*-hexane:AcOEt = 1:5); ^{1}H NMR (300 MHz, $CDCl_3$) δ 7.20–7.40 (m, 10H), 5.25 (br s, 1H), 5.14 (s, 1H), 5.12 (s, 1H), 4.79 (d, 0.5H, J = 5.5 Hz), 4.78 (d, 0.5H, J = 5.5 Hz), 4.63–4.69 (m, 1H), 4.33–4.38 (m, 0.5H), 4.16–4.20 (m, 0.5H), 3.80–3.84 (m, 0.5H), 3.65–3.70 (m, 0.5H), 3.14–3.24 (m, 0.5H), 2.93–3.02 (m, 2H), 2.76–2.88 (m, 1.5H), 2.54–2.65 (m, 1H), 1.55–1.98 (m, 4H); ^{13}C NMR (75.5 MHz, $CDCl_3$) δ 173.7, 173.4, 164.4, 164.3, 156.9, 135.8, 135.8, 135.7, 129.1, 129.0, 128.6, 128.3, 128.3, 128.1, 127.3, 76.8, 76.6, 66.5, 55.3, 44.8, 44.5, 42.0, 41.8, 41.0, 41.0, 40.9, 40.3, 28.4, 28.2, 27.5, 27.5; $[\alpha]_D^{27}$ −91.2 (c 1.281, $CHCl_3$); IR (KBr) 3452, 3036, 3007, 1771, 1730, 1653, 1456, 1387, 1313, 1271, 1238, 1209, 1173, 1038, 1011, 756, 737, 698, 667 cm^{-1}; HRMS (EI$^+$): m/z 422.1845 for [M$^+$] (calcd 422.1842 for $C_{24}H_{26}N_2O_5$); elemental analysis calcd for $C_{24}H_{26}N_2O_5$: C, 68.23; H, 6.20; N, 6.63. Found: C, 67.99; H, 6.20; N, 6.55.
14. Cutugno, S.; Martelli, G.; Negro, L.; Savoia, D. *Eur. J. Org. Chem.* **2001**, 517–522.
15. General procedure for solution-phase chiral synthesis of α-alkylated carboxylic acids using compound **5**: Briefly, to a solution of **5** in THF, was added LDA (1.2 equiv) dropwise at −78 °C. After stirring for 30 min, the solution was quenched with the alkyl halide (10 equiv), and warmed to 0 °C in 3 h with stirring. Stirring again with saturated NH_4Cl solution followed by the extraction with AcOEt, washing the organic layer with water and brine, drying over Na_2SO_4, and finally the removal of the solvent gave **6**. Without further purification, the LiOOH hydrolysis of **6** was carried out according to the previous report,[16] and then the product was purified by preparative TLC for removing nonalkylated carboxylic acid. The resultant pure **7** was next coupled with (*S*)-phenylethylamine by the EDC–HOBt method to determine the enantiomeric excesses of the α-alkylated carboxylic acids **7** by HPLC.
16. (a) Evans, D. A.; Britton, T. C.; Ellman, J. A. *Tetrahedron Lett.* **1987**, *28*, 6141–6144; (b) Evans, D. A.; Ellman, J. A. *J. Am. Chem. Soc.* **1989**, *111*, 1063–1072.
17. Atherton, E.; Benoiton, N. L.; Brown, E.; Sheppard, R. C.; Williams, B. J. *J. Chem. Soc., Chem. Commun.* **1981**, 336–337.
18. Ho, G.-J.; Mathre, D. J. *J. Org. Chem.* **1995**, *60*, 2271–2273.
19. Mukaiyama, T. *Angew. Chem., Int. Ed. Engl.* **1979**, *18*, 707–721.
20. The crude product **7** was purified by preparative TLC to remove nonalkylated carboxylic acid. The relatively lower yield (38–54%) that was observed in the solid-phase method was due to the fact that the yield includes the four step reaction from Wang resin to the final product **7**. The yield for two steps (alkylation and hydrolysis) is likely to be similar to that of the solution-phase method.
21. Kim, D. H.; Li, Z.-H.; Lee, S. S.; Park, J.; Chung, S. J. *Bioorg. Med. Chem.* **1998**, *6*, 239–249.

PROTEINS: Structure, Function, and Bioinformatics 55:594–602 (2004)

A Structural and Thermodynamic Escape Mechanism from a Drug Resistant Mutation of the HIV-1 Protease

Sonia Vega,[1†] Lin-Woo Kang,[2†] Adrian Velazquez-Campoy,[1] Yoshiaki Kiso,[3] L. Mario Amzel,[2] and Ernesto Freire[1*]
[1]*Department of Biology, The Johns Hopkins University, Baltimore, MD 21218*
[2]*Department of Biophysics and Biophysical Chemistry, The Johns Hopkins University School of Medicine, Baltimore, MD 21218*
[3]*Department of Medicinal Chemistry, Center for Frontier Research in Medicinal Science, Kyoto Pharmaceutical University, Yamashina-ku, Kyoto 607-8412, Japan*

ABSTRACT **The efficacy of HIV-1 protease inhibition therapies is often compromised by the appearance of mutations in the protease molecule that lower the binding affinity of inhibitors while maintaining viable catalytic activity and substrate affinity. The V82F/I84V double mutation is located within the binding site cavity and affects all protease inhibitors in clinical use. KNI-764, a second-generation inhibitor currently under development, maintains significant potency against this mutation by entropically compensating for enthalpic losses, thus minimizing the loss in binding affinity. KNI-577 differs from KNI-764 by a single functional group critical to the inhibitor response to the protease mutation. This single difference changes the response of the two inhibitors to the mutation by one order of magnitude. Accordingly, a structural understanding of the inhibitor response will provide important guidelines for the design of inhibitors that are less susceptible to mutations conveying drug resistance. The structures of the two compounds bound to the wild type and V82F/I84V HIV-1 protease have been determined by X-ray crystallography at 2.0 Å resolution. The presence of two asymmetric functional groups, linked by rotatable bonds to the inhibitor scaffold, allows KNI-764 to adapt to the mutated binding site cavity more readily than KNI-577, with a single asymmetric group. Both inhibitors lose about 2.5 kcal/mol in binding enthalpy when facing the drug-resistant mutant protease; however KNI-764 gains binding entropy while KNI-577 loses binding entropy. The gain in binding entropy by KNI-764 accounts for its low susceptibility to the drug-resistant mutation. The heat capacity change associated with binding becomes more negative when KNI-764 binds to the mutant protease, consistent with increased desolvation. With KNI-577, the opposite effect is observed. Structurally, the crystallographic B factors increase for KNI-764 when it is bound to the drug-resistant mutant. The opposite is observed for KNI-577. Consistent with these observations, it appears that KNI-764 is able to gain binding entropy by a two-fold mechanism: it gains solvation entropy by burying itself deeper within the binding pocket and gains conformational entropy by losing interaction with the protease. Proteins 2004;55:594–602.**

Key words: HIV protease; drug resistance; thermodynamics; crystallography; calorimetry

INTRODUCTION

A significant obstacle to the efficacy of drugs directed against viral targets is the appearance of drug-resistant mutations in the targeted molecules. The clinical use of HIV-1 protease inhibitors in antiretroviral therapies clearly illustrates the capacity of the virus to mutate and develop strains carrying mutant protease molecules with a significantly lower affinity for the inhibitors while maintaining sufficient catalytic activity for viral reproduction.[1–9] To be effective against a wide spectrum of protease variants, an inhibitor needs to exhibit an extremely high activity against wild-type protease and be affected only mildly by protease mutations. Ideally, an inhibitor should have a binding affinity in the 1–50 pM range against the wild type and be affected by mutations by a factor of 100 or less.[10–12] The extremely high activity required against the wild type can only be achieved if both enthalpy and entropy contribute favorably to the Gibbs energy.

In this article we describe the high resolution crystallographic structures of the complexes of two chemically and structurally similar HIV-1 protease inhibitors (KNI-764 and KNI-577) with the wild type HIV-1 protease and a common mutation associated with drug resistance to protease inhibitors currently in clinical use (V82F/I84V). Both inhibitors bind to the wild-type HIV-1 protease with high affinity but respond differently to the mutation.[10] Despite their chemical and structural similarities, KNI-577 loses binding affinity by a factor of 200 while KNI-764 loses binding affinity only by a factor of 20.[10] By combining high resolution structural data with binding thermodynamic results for both inhibitors against wild type and mutant protease, we attempt to understand the mechanism by

Grant sponsor: National Institutes of Health; Grant numbers: GM57144 (E.F.) and GM45540 (L.M.A.).

*Correspondence to: Ernesto Freire, Department of Biology, The Johns Hopkins University, 3400 North Charles, Baltimore, MD 21218, USA. Email: ef@jhu.edu.

†Sonia Vega and Lin-Woo Kang contributed equally to this paper.

Received 18 August 2003; 3 November 2003; Accepted 18 November 2003

Published online 1 April 2004 in Wiley InterScience (www.interscience.wiley.com). DOI: 10.1002/prot.20069

which an inhibitor can evade the negative effects of mutations. This mechanism could delineate a general strategy for the design of drug molecules that are more resistant to the effect of target mutations.

METHODS

Protein Purification

Protease expression, purification and refolding were performed as described before.[25,26] Briefly, plasmid-encoded HIV-1 protease was expressed as inclusion bodies in *E. coli* BL21(DE3). Cells were suspended in extraction buffer (20 m*M* Tris, 1 m*M* EDTA, 10 m*M* 2-ME, pH 7.5) and broken with two passes through a French pressure cell (≥16000 psi). Cell-debris and protease-containing inclusion bodies were collected by centrifugation (20,000 g for 20 min at 4°C). Inclusion bodies were washed with three buffers. Each wash consisted of re-suspension (glass homogenizer, sonication) and centrifugation (20,000 g for 20 min at 4°C). In each step a different washing buffer was employed: buffer-1 (25 m*M* Tris, 2.5 m*M* EDTA, 0.5*M* NaCl, 1 m*M* Gly-Gly, 50 m*M* 2-ME, pH 7.0); buffer-2 (25 m*M* Tris, 2.5 m*M* EDTA, 0.5*M* NaCl, 1 m*M* Gly-Gly, 50 m*M* 2-ME, 1*M* urea, pH 7.0); buffer-3 (25 m*M* Tris, 1 m*M* EDTA, 1 m*M* Gly-Gly, 50 m*M* 2-ME, pH 7.0). Protease was solubilized in 25 m*M* Tris, 1 m*M* EDTA, 5 m*M* NaCl, 1 m*M* Gly-Gly, 50 m*M* 2-ME, 9*M* urea, pH 9.0, clarified by centrifugation and applied directly to an anion exchange Q-Sepharose column (Q-Sepharose HP, Pharmacia) previously equilibrated with the same buffer. The protease was passed through the column and then acidified by adding formic acid to 25 m*M* immediately upon elution from the column. Precipitation of a significant amount of the contaminants occurred upon acidification. Protease-containing fractions were pooled, concentrated and stored at 4°C at 5–10 mg/mL.

The HIV-1 protease was folded by ten-fold stepwise dilution into 10 m*M* formic acid at 0°C. The pH was gradually increased to 3.8, and then the temperature was raised to 30°C. Sodium acetate (pH 5.0) was added to increase the pH to 5.0, and the protein was concentrated. Folded protease was desalted into 1 m*M* sodium acetate at pH 5.0 using a gel filtration column (PD-10, Pharmacia) and stored at either 4°C or −20°C (≥2.5 mg/ml) without loss of activity over several weeks. After folding, the protease was estimated to be ≥99% pure.

Activity of the refolded protein was assessed by active site titration, performed by isothermal titration calorimetry (VP-ITC, Microcal LLC, Northampton MA) as described before.[11,17]

Isothermal Titration Calorimetry

Isothermal titration calorimetry experiments were carried out using a high precision VP-ITC titration calorimetric system (Microcal Inc, Northampton, MA). The enzyme solution (10–20 μ*M* dimer) in the calorimetric cell was titrated with KNI-764, KNI-577 or acetyl-pepstatin (0.15-0.3 m*M*) dissolved in the same buffer (10 m*M*, DMSO 2% v/v). In displacement titration experiments (see below), inhibitors were injected into the calorimetric cell containing the protein pre-bound to a weak inhibitor (acetyl-pepstatin) as described before.[11,12,26] The concentration of acetyl-pepstatin in the titration cell was 0.2 m*M*. Protein and inhibitor solutions were properly degassed and carefully loaded into the cells to avoid bubble formation during stirring. Exhaustive cleaning of the cells was undertaken before each experiment. The heat evolved after each ligand injection was obtained from the integral of the calorimetric signal. The heat due to the binding reaction between the inhibitor and the enzyme was obtained as the difference between the heat of reaction and the corresponding heat of dilution. Blank experiments were performed by injecting the inhibitor into buffer solution to confirm the absence of self-association effects in the ligand.

The binding enthalpy was measured at two pH values (3.8 and 5.0) using several buffers differing in ionization enthalpy (acetate 0.12 kcal/mol, MES 3.72 kcal/mol, ACES 7.51 kcal/mol, cacodylate −0.47 kcal/mol, formate −0.05 kcal/mol, glycine 1.07 kcal/mol, cytidine 4.50 kcal/mol). The extension and contribution of protonation/deprotonation processes to the binding were assessed by determination of the pH-dependence of the binding enthalpy. The pH values were selected according to a previous work with KNI-272, another allophenylnorstatine-based inhibitor, which exhibits maximal and minimal proton release upon binding at these pH values.[17] The binding enthalpy of both KNI-764 and KNI-577 showed no dependence on the ionization enthalpy of the buffer, indicating no net proton exchange under the conditions of these experiments.

Displacement Isothermal Titration Calorimetry

KNI-764 and KNI-577 are tightly-binding inhibitors ($K_d < 1$ n*M*) of the HIV-1 protease, and therefore standard titration experiments do not provide accurate estimates of the binding affinity, even though the binding enthalpy can be determined with high accuracy. In order to overcome this impediment, calorimetric displacement titrations were carried out, allowing for the determination of the affinity and enthalpy of binding.[11,12,26,27] In calorimetric displacement titrations, the high-affinity inhibitor is titrated into a protease sample pre-bound to a weaker inhibitor. Under these conditions, the apparent binding affinity of the tight inhibitor diminishes in a manner proportional to the affinity and free concentration of the weak inhibitor and becomes calorimetrically measurable. Two calorimetric titrations are required to solve the binding equations and determine the binding affinity and binding enthalpy of the tightly-binding inhibitor: the titration of the weak inhibitor into the protease and the titration of the high-affinity inhibitor into the protease pre-bound to the weak inhibitor. Analysis of the data was performed using software developed in this laboratory as described previously.[11] The change in heat capacity, the temperature derivative of the binding enthalpy, was determined by performing titrations at different temperatures (Fig. 1). It can be calculated as the slope from the linear regression of binding enthalpy versus temperature.

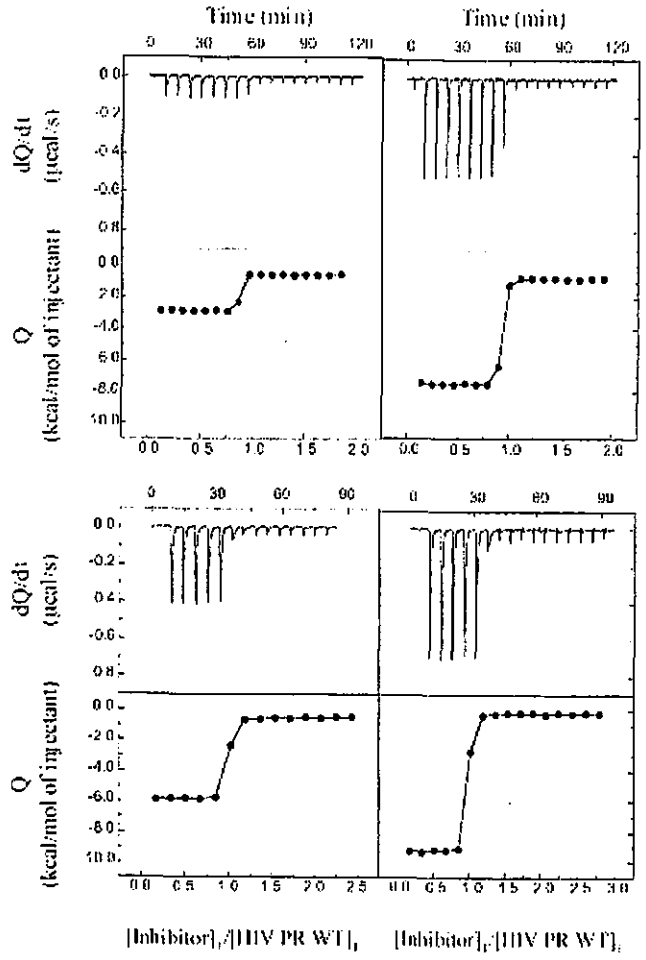

Figure 1. Typical calorimetric titrations of KNI-577 (top) and KNI-764 (bottom) into a solution of HIV-1 wild-type protease. The experiments were performed in sodium acetate 10 m*M*, pH 5.0 and DMSO 2%. The experiments on the left panels were performed at 20°C and on the right panels at 30°C. Additional experiments at 25°C were also used to determine the heat capacity change for each inhibitor against each protease used in these studies.

Crystallization

Crystals of HIV-1 protease WT were grown in hanging drops of equal amounts of reservoir solution (100 m*M* MOPS pH 7.0, 250 m*M* NaCl, 10 m*M* DTT, 3 m*M* NaN_3) and protein solution (6 mg/mL, 1 m*M* sodium acetate pH 5.0, 2 m*M* NaCl). Previously, the inhibitor (KNI-764 or KNI-577) was added to the protein solution from a concentrated (≈15 m*M*) stock solution in 100% DMSO to a final ratio of protease to inhibitor of 1:2. The drops were equilibrated against a volume of 1 mL of reservoir solution. DMSO was added to the reservoir to a final percentage equal to the one expected in the drops after equilibration (≈7%). Crystals grew in 1-2 days at 4°C.

Direct attempts to crystallize the V82F/I84V double mutant protease with the inhibitors KNI-764 and KNI-577 were not successful. In order to overcome this difficulty, crystallization was made with acetyl-pepstatin under the same conditions as reported above for the protease WT. Because acetyl-pepstatin is a less potent inhibitor than the KNI's, the ratio of fprotease to inhibitor was increased up to 1:10. Because the stock solution of acetyl-pepstatin (≈8 m*M*) was made in pure water, no DMSO was added to the reservoir. Crystals grew in 1-2 days at 4°C.

Once double mutant protease crystallized with acetyl-pepstatin, a ligand replacement technique was employed to obtain crystals of double mutant with KNI-764 and KNI-577. Crystals of protease with acetyl-pepstatin were washed and soaked in drops made with equal volumes of precipitant buffer and KNI-764 or KNI-577 solution (at 1 m*M* sodium acetate pH 5.0, 2 m*M* NaCl). Again, DMSO was added in the reservoir to the same percentage as the one expected in the drops after equilibration (≈7%).

Structure Determination

Four different data sets (wild-type and mutant HIV protease with either KNI-764 or KNI-577) were collected to 2.0 Å resolution on a RAxis IV Image Plate system using a rotating anode source equipped with Osmic mirrors (Molecular Structure Corporation, Texas). Diffraction data were processed with DENZO and SCALEPACK.[28] Autoindexing and consideration of systematically absent reflections revealed that the crystals belong to space group $P2_12_12$, unit-cell parameters a = 57.7 Å, b = 85.8 Å, c = 46.5 Å with two monomers in the asymmetric unit. Molecular replacement searches using the coordinates of the HIV protease from the crystal structure of the complex with inhibitor KNI-272 (PDB ID: 1HPX) as the search molecule yielded a clear solution.

An electron density map, calculated with phases based on the protein only, showed well-resolved density that allowed fitting all portions of the inhibitor as well as the side chains of mutated residues. Models consisting of protein coordinates plus those of the inhibitors were refined using the Crystallography and NMR System (CNS)[29] with a residual target that did not include non-crystallographic symmetry restraints. Rebuilding and correction of the models was guided by σA-corrected 2Fo-Fc electron density maps. R and R-free (calculated with randomly selected 10% of the reflections) were used to monitor refinement of the model.[30] The quality of the structures was assessed with the program PROCHECK.[31] The final refinement and model statistics are shown in Table I.

Coordinates

The coordinates have been deposited in the Protein Data Bank (accession codes 1MRW and 1MRX for the complex of KNI-577 with the wild type and drug resistant mutants, and 1MSM and 1MSN for the complex of KNI-764 with the wild type and drug resistant mutants, respectively).

RESULTS AND DISCUSSION

The Inhibitors

KNI-577 and KNI-764 are highly potent inhibitors of HIV-1 protease with K_i values in the subnanomolar range against wild-type enzyme.[10] At 25°C, KNI-577 and KNI-764 bind to wild-type protease with K_d values of 0.2 and 0.03 n*M* respectively. Structurally, the two inhibitors are identical except for the functional group at the P2′ position

TABLE I. Statistics for Data Collection and Refinement

Data sets	HIV Protease WT	HIV Protease 82/84MT	HIV Protease WT	HIV Protease 82/84MT
Inhibitor	KNI-764	KNI-764	KNI-577	KNI-577
Space group		P21212		
Cell constants		a = 58.1Å b = 86.0Å c = 46.5Å		
Resolution	20–2.0Å	20–2.0Å	20–2.0Å	20–2.0Å
Observed reflections	122330	121342	126994	81856
Unique reflections	15861	15875	16090	13461
Completeness (%)	97.7	98.5	98.3	82.9
(High resolution shell)	87.7	95.9	88.7	75.8
R sym[1]	0.067	0.078	0.103	0.072
Refinement				
R crystal/R free	0.209/0.236	0.222/0.249	0.218/0.246	0.208/0.250
Model composition[2]				
Amino acids (atoms)	198 (1516)	198 (1522)	198 (1516)	198 (1522)
Ligands (atoms)				
KNI-764 or KNI-577	1 (41)	1 (41)	1 (37)	1 (37)
Waters	147	123	112	128
Total atoms	1704	1686	1665	1687
Stereochemistry[3]				
r.m.s. Bond length (Å)	0.0063	0.0066	0.0065	0.0062
r.m.s. Angles (°)	1.22	1.28	1.31	1.23
<B-factor protein>	24.2	27.2	28.3	26.2
<B-factor water>	31.5	35.2	33.6	34.1
<B-factor ligand>	17.7	25.6	26.0	22.2

[1] $R_{sym} = (\Sigma|I_{hkl} - \langle I \rangle|)/(\Sigma I_{hkl})$, where I_{hkl} is the observed intensity and $\langle I \rangle$ is the average intensity obtained from multiple observations of symmetry-related reflections.
[2] Model composition shows two monomers in asymmetric unit.
[3] Over 90% of main chain dihedrals fall within the 'most allowed regions' of the Ramachandran plot.

(see Fig. 2). In KNI-577, this position is occupied by a symmetric t-butylamide group, whereas in KNI-764 the position is occupied by a larger methylbenzylamide group. In KNI-577, there is one rotatable bond between the amide and the t-butyl group, and in KNI-764 there are two rotatable bonds between the amide and the phenyl ring. Both inhibitors bind to the protease in a process favored by enthalpic and entropic interactions.[10] At 25°C, the differences in affinity are due to the more favorable binding enthalpy of KNI-764 (2.9 kcal/mol) (see Fig. 1 and Table II), suggesting that this inhibitor establishes better interactions with wild-type protease than does KNI-577. KNI-577 on the other hand, exhibits a more favorable entropic contribution to the Gibbs energy of binding than does KNI-764 (1.8 kcal/mol), but this is not sufficient to overcome the more favorable binding enthalpy of KNI-764.

Analysis of the crystal structures of KNI-577 and KNI-764 bound to wild-type protease reveals that a group of conserved water molecules at the inhibitor–protein interface (Fig. 3) plays a crucial role in establishing a tight atomic packing density within the binding cavity. These water molecules have been shown to be immobilized within NMR timescales in the case of another allophenylnorstatine (Apns)-based inhibitor.[13] Also, because these water molecules establish important hydrogen bonds and van der Waals contacts between inhibitor and protein, they have been shown to contribute significantly to the observed binding enthalpy.[14]

Inhibitor Response to V82F/I84V Drug Resistant Mutation

Despite their structural similarities, the two inhibitors respond differently to the same drug resistant mutation V82F/I84V. Figures 3 and 4 show the structures of the inhibitors bound to wild-type and V82F/I84V protease mutant. Previously, Reiling et al[15] determined the structure of KNI-764 with a version of wild-type protease differing in six residues from the one reported here.

Although the structures of the four complexes reported here are highly similar, small localized differences are observed among them (Figs. 3-4). In all complexes, both monomers (A and B) of the HIV-1 protease interact with the inhibitor. In the case of the complexes with KNI-764, residue 82 (monomer A) interacts with the phenyl ring of the inhibitor, and residue 84 (monomer A) interacts with the same phenyl ring as well as with the methylbenzylamide moiety. In monomer B, residue 84 interacts with the dimethylthioproline group, but residue 82 does not interact with the inhibitor. As a result of these interactions, the substitutions present in the mutant (V82F/I84V) bring about small but significant changes in both the position and the conformation of the inhibitor. The largest changes involve movements of the aromatic rings of the inhibitor. The rotation in the plane of the ring of the methylbenzylamide by about 25° results in displacements of several atoms by up to 1.3 Å. Displacements of the same magnitude are observed for the 3-hydroxy-2-methylbenzoyl moiety, and

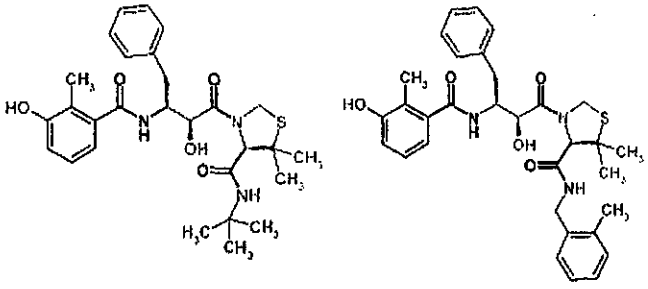

Figure 2. The chemical structure of KNI-577 (left) and KNI-764 (right). Both inhibitors share the same allophenyl-norstatine scaffold at the P1 position (red) and the same functional groups at the P2 (blue) and P1' positions (green). The only difference is at the P2' position (magenta).

Figure 4. Superposition of the complexes of KNI-764 (left) and KNI-577 (right) bound to wild-type (cyan) and double mutant (purple) protease.

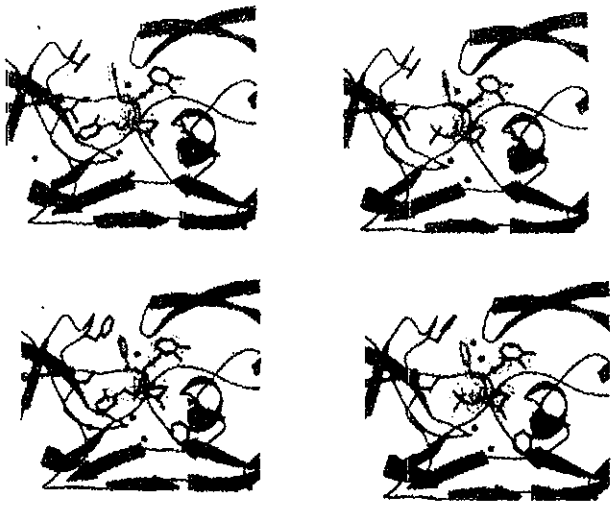

Figure 3. Complexes of KNI-764 and KNI-577 bound to wild-type (upper panels) and V82F/I84V double mutant (lower panels) HIV-1 protease. The electronic densities of KNI-764 (left panels) and KNI-577 (right panels) bound to the protease are shown. Water molecules considered in the structure-based thermodynamic analysis are shown in red.

smaller changes occur for the phenyl ring in Apns and the dimethylthioproline moieties.

In the complexes with KNI-577 all of the differences between wild type and mutant are smaller than those observed with KNI-764 with one exception: the displacement of the phenyl ring in Apns is significantly larger than in the other complex. In the rest of the structure, including the 3-hydroxy-2-methylbenzoyl moiety and the dimethylthioproline, the changes are in general less than 0.3 Å. The *t*-butyl group, which in KNI-577 replaces the methylbenzylamide of KNI-764, hardly moves at all compared to the large movement experienced by the methylbenzylamide of KNI-764. The effect of these structural changes on the differences in thermodynamic properties of the four complexes is discussed below.

Thermodynamic Response to Drug Resistant Mutation

KNI-764 and KNI-577 lose significant enthalpic interactions (2.3 and 2.6 kcal/mol, respectively) when facing the drug resistant mutant (Table II). However, KNI-764 is able to partially compensate for the loss in binding enthalpy by a gain in binding entropy. When the effects of the enthalpy loss and the entropy gain are combined, it becomes evident why KNI-764 loses affinity by only a factor of 25 while KNI-577 loses affinity by a factor of 260. In absolute terms, KNI-764 maintains a nanomolar affinity against the drug-resistant mutant while the affinity of KNI-577 becomes close to 100 *nM*. In fact, KNI-764 inhibits the V82F/I84V drug-resistant mutant with an affinity similar to that of first-generation protease inhibitors against wild-type protease.[9–11] The affinity of KNI-577, on the other hand, weakens below the level required for effective inhibition.

Isothermal titration calorimetric experiments performed at different temperatures (Fig. 5) indicate that the binding of both inhibitors is associated with a negative change in heat capacity. The magnitude of the heat capacity change is different for each inhibitor, and their response to the drug-resistant mutant is also different. KNI-764 exhibits a ΔC_p of -360 ± 20 cal K^{-1} mol^{-1} against the wild type and -390 ± 15 cal K^{-1} mol^{-1} against the mutant. KNI-577, on the other hand, exhibits a ΔC_p of -420 ± 20 cal K^{-1} mol^{-1} against the wild type and -380 ± 20 cal K^{-1} mol^{-1} against the mutant, i.e. the ΔC_p value for KNI-764 decreases while the ΔC_p value for KNI-577 increases.

The solvent-accessible surface areas of KNI-577 and KNI-764 are 760 and 820 Å^2 respectively, of which 598 and 657 Å^2 correspond to non-polar surface. Upon binding to the wild-type enzyme, KNI-577 buries 573 Å^2 of its non-polar surface and 163 Å^2 of its polar surface. KNI-764, on the other hand, buries 607 Å^2 of its non-polar surface and 162 Å^2 of its polar surface. Against the V82F/I84V mutant KNI-577 buries 558 Å^2 of its non-polar surface, while KNI-764 buries 619 Å^2. The amount of buried polar surface remains unchanged for both inhibitors. The actual increase in the non-polar surface area buried by KNI-764 against the mutant protein reveals the adaptability of this inhibitor by its capacity to bury itself deeper into the mutant binding cavity. At the thermodynamic level, this structural feature provides an important contribution to the compensating entropy change. The opposite effect is seen with KNI-577, which buries a smaller non-polar surface area against the mutant protease.

TABLE II. Binding Thermodynamics of Inhibitors to Wild Type and V82F/I84V Drug-Resistant Mutant at 25°C

	ΔG (cal/mol)	ΔH (cal/mol)	$-T\Delta S$ (cal/mol)	ΔC_p [cal k^{-1} mol^{-1}]
KNI-764 → WT	−14300 ± 100	−7600 ± 300	−6700 ± 300	−360 ± 20
KNI-764 → V82F/I84V	−12400 ± 100	−5300 ± 200	−7100 ± 200	−390 ± 15
KNI-577 → WT	−13200 ± 100	−4700 ± 200	−8500 ± 200	−420 ± 20
KNI-577 → V82F/I84V	−9900 ± 100	−2100 ± 200	−7800 ± 200	−380 ± 20

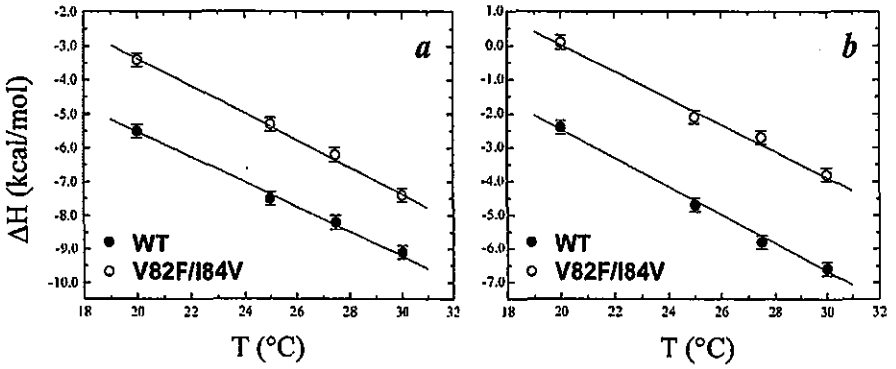

Figure 5. Determination of the change in heat capacity (ΔC_p) upon binding for a) KNI-764 and b) KNI-577 to wild-type and V82F/I84V mutant proteases. ΔC_p is equal to the slope of the enthalpy versus temperature plot.

The loss in binding enthalpy against the mutant experienced by both inhibitors can be explained in terms of the loss of van der Waals contacts when the inhibitors, selected against the wild-type enzyme, face an altered binding cavity. The gain in entropy experienced by KNI-764 could originate from several factors. An increase in solvation entropy would be consistent with the more negative heat capacity change observed with the mutant.[16] Another potential source of compensation is an increase in conformational entropy. One can envision a situation in which the loss of interactions is accompanied by an increase in the conformational degree of freedom of ligand and protein, especially if the loss occurs in non-conformationally constrained regions of the inhibitor. In this respect we observe an increase in the crystallographic B-factors for the KNI-764/mutant complex, while the opposite is true for KNI-577.

Structure-Based Thermodynamic Analysis

The crystallographic structures and the thermodynamic data discussed here indicate that the partial compensation of the binding enthalpy loss with an actual gain in binding entropy provides the thermodynamic mechanism to escape the deleterious effects of the V82F/I84V drug resistant mutation, and that this behavior originates from the better adaptability of KNI-764 to the binding site distortions introduced by the mutations. Recently, a refined structural parameterization of the enthalpy change associated with the binding of small ligands was presented.[14] Four set of parameters were considered to be important for a quantitative account of the binding enthalpy: (1) the interactions between ligand and protein, reflected in changes in solvent accessible surface areas for ligand and protein; (2) the conformational change associated with binding; (3) the presence of water molecules at the protein–ligand interface (a cutoff of 6 Å for completely buried water molecules was reported); and (4) any effects due to protonation/deprotonation associated with ligand binding.

In order to assess whether the thermodynamic response can be explained quantitatively in terms of structure, a parameterization of the binding energy developed previously was utilized. If the parameters reported by Luque and Freire[14] [$\Delta H(25) = \Delta H_{conf} - 7.35\Delta ASA_{np} + 31.06 \times \Delta ASA_{pol}$] are applied to the four structures presented here, the results shown in Figure 6 are obtained. In all cases, the reported conformational enthalpy change (ΔH_{conf}) of 5900 cal/mol for the protease molecule upon binding was used.[14] Protonation effects for these two inhibitors do not contribute significantly to the binding enthalpy, as demonstrated by microcalorimetric titrations performed with buffers having different heats of ionization (data not shown).[17] According to the published report,[14] water molecules at protein–inhibitor interface contribute significantly to the binding enthalpy. In the KNI-764 complex with the wild type, six water molecules are buried within 6 Å of the inhibitor (2, 5, 10, 27, 99, 148) while in the complex with the drug resistant mutant only 5 water molecules (11, 22, 47, 91, 111) are buried. In the complex of KNI-577 with the wild–type protease, five water molecules are buried within 6 Å (1, 5, 6, 49, 84), and the same number are found with the resistant mutant (6, 7 57, 87, 123). The water molecules that satisfy the published criteria are shown in Figure 3. As shown in Figure 6, the parameterization predicts the binding enthalpies within 1.4 kcal/mol of the experimental value. For KNI-577 against the mutant protease, the error is somewhat larger and amounts to ≈2 kcal/mol. In all cases, the loss of binding enthalpy against the

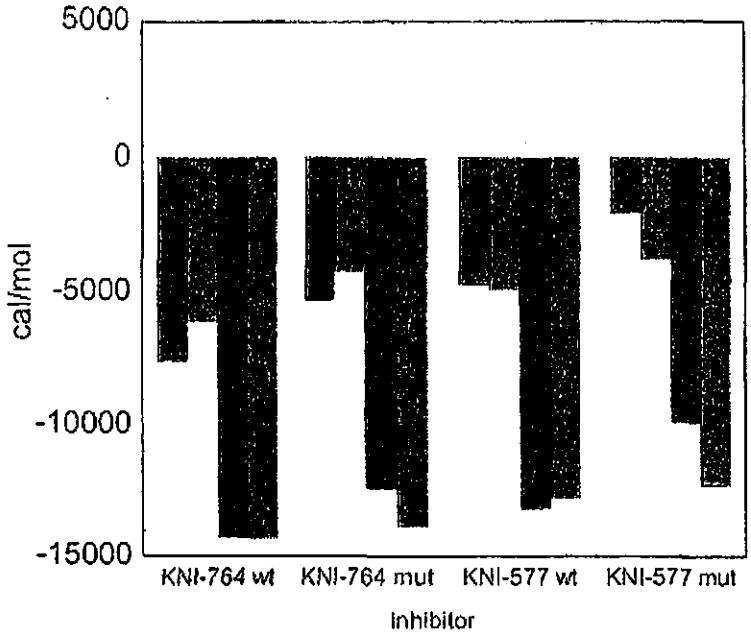

Figure 6. Experimental and calculated binding enthalpies (open and hatched bars) and binding Gibbs energies (solid and crossed bars). The standard deviation between experimental and calculated enthalpies is 1.4 kcal/mol. The standard deviation between experimental and calculated Gibbs energies is 1.3 kcal/mol.

TABLE III. Structure-Based Thermodynamic Analysis of Inhibitor Complexes with Wild Type and Drug-Resistant Mutant at 25°C

	KNI-764 wild type	KNI-764 mutant	KNI-577 wild type	KNI-577 mutant
ΔASA_{pol}[1] Å^2	−588 (−322)	−535 (−333)	−527 (−337)	−499 (−325)
ΔASA_{np}[1] Å^2	−848 (−889)	−884 (−932)	−756 (−814)	−789 (−829)
ΔH_{int} kcal/mol	−12.0	−10.1	−10.8	−9.7
$-T\Delta S_{solv}$ kcal/mol	−23.3	−25.0	−20.7	−22.1
$-T\Delta S_{conf}$ kcal/mol	18.4	18.5	16.1	16.8
$-T\Delta S_{rt}$ kcal/mol	2.4	2.4	2.4	2.4
ΔG_{el} kcal/mol	0.2	0.4	0.2	0.3
ΔG_{calc} kcal/mol	−14.3	−13.8	−12.8	−12.3

[1]The changes in solvent accessible surface area include the contributions due to the water molecules at the protein/inhibitor interface. The number in parenthesis represent the changes in solvent accessible surface areas calculated without taking into consideration the water molecules at the protein/inhibitor interface. ΔH_{int} is the intrinsic binding enthalpy assuming that the protease is in the same conformation in the free and bound states. The experimental enthalpy is calculated by adding the enthalpy corresponding to the change in conformation (5.9 kcal/mol) to this value. ΔS_{solv} and ΔS_{conf} are the calculated changes in solvation and conformational entropy, respectively. ΔS_{rt} correspond to the loss of translational degrees of freedom and is approximated by the cratic entropy[16]. ΔG_{el} is the coulombic contribution to the Gibbs energy[16].

drug resistant mutant is correctly predicted. Each water molecule optimizes the atomic packing density between inhibitor and protein and contributes on the order of −1.2 kcal/mol to the binding enthalpy. Against the drug resistant mutation, KNI-764 loses one of the buried water molecules but is able to partially compensate for this loss by accommodating itself within the binding pocket. It ends up suffering a smaller enthalpy loss than KNI-577, which maintains the same number of buried water molecules with the mutant.

The global changes in solvent accessible surface area are shown in Table III. These changes include the sum protein contributions, as well as those made by the inhibitor, taking into consideration the water molecules at the protein–inhibitor interface. For comparison, the global changes calculated without considering the water molecules are also shown. It is clear that the inclusion of the water molecules makes a significant contribution, especially to the polar surface that is buried upon binding. It is also seen that against the mutant the enthalpy loss originates from a diminished number of polar contacts reflected in a loss in buried polar surface area coupled to a gain in buried nonpolar surface area. The larger error observed for KNI-577 against the mutant protease could be due to an overestimation of the number of water molecules buried at the interface. As a result of this error, KNI-577 is predicted to lose ≈1 kcal/mol less than KNI-764 against the mutant. In the